

Excited-State Photophysics of Hypericin and Its Hexamethoxy Analog: Intramolecular Proton Transfer as a Nonradiative Process in Hypericin

D. S. English, W. Zhang, G. A. Kraus,* and J. W. Petrich*

Contribution from the Department of Chemistry, Iowa State University, Ames, Iowa 50011

Received July 17, 1996[⊗]

Abstract: The excited-state photophysics of the light induced antiviral agent, hypericin, are compared with those of its methylated analog, hexamethoxyhypericin. This comparison is instructive in understanding both the ground- and the excited-state properties of hypericin. That the hexamethoxy analog has no labile protons that can be transferred, that it cannot protonate its own carbonyl groups, that it has a reduced fluorescence quantum yield and lifetime with respect to hypericin, and that it exhibits no stimulated emission or, more specifically, rise time in stimulated emission completely support our emerging model of the hypericin photophysics. The results are consistent with the presence of intramolecular excited-state proton transfer in hypericin but not in its methylated analog.

Introduction

Interest in the polycyclic quinone, hypericin (Figure 1a) was spawned by the discovery that it possesses extremely high toxicity toward certain viruses, including HIV and that this toxicity absolutely requires light.^{1–3} Hypericin is also very similar in structure to the stentorin chromophore that confers phototactic and photophobic responses to protozoan ciliates.⁴ The interaction of light with hypericin and hypericin-like chromophores is clearly of fundamental biological importance. In order to understand and eventually to exploit these properties of hypericin, it is essential to elucidate its nonradiative excited-state processes. We have undertaken this task using the tools of ultrafast time-resolved absorption spectroscopy and have presented our results in a series of articles.^{5–13}

The argument for the presence of intramolecular excited-state proton transfer in hypericin is as follows. The hypericin analog

* To whom correspondence should be addressed.

⊗ Abstract published in *Advance ACS Abstracts*, March 15, 1997.

(1) Carpenter, S.; Kraus, G. A. *Photochem. Photobiol.* **1991**, *53*, 169–174.

(2) Meruelo, D.; Lavie, G.; Lavie, D. *Proc. Natl. Acad. Sci. U.S.A.* **1988**, *85*, 5230–5234. Degar, S.; Prince, A. M.; Pascual, D.; Lavie, G.; Levin, B.; Mazur, Y.; Lavie, D.; Ehrlich, L. S.; Carter, C.; Meruelo, D. *AIDS Res. Hum. Retroviruses* **1992**, *8*, 1929–1936. Lenard, J.; Rabson, A.; Vanderoef, R. *Proc. Natl. Acad. Sci. U.S.A.* **1993**, *90*, 158–162. Meruelo, D.; Degar, S.; Nuria, A.; Mazur, Y.; Lavie, D.; Levin, B.; Lavie, G. In *Natural Products as Antiviral Agents*; Chu, C. K., and Cutler, H. G., Eds. Plenum Press: New York, 1992 pp 91–119, and references therein.

(3) Diwu, Z. *Photochem. Photobiol.* **1995**, *61*, 529–539.

(4) Durán, N.; Song, P.-S. *Photochem. Photobiol.* **1986**, *43*, 677–680. Tao, N.; Orlando, M.; Hyon, J. S.; Gross, M. L.; Song, P.-S. *J. Am. Chem. Soc.* **1993**, *115*, 2526.

(5) Gai, F.; Fehr, M. J.; Petrich, J. W. *J. Am. Chem. Soc.* **1993**, *115*, 3384–3385.

(6) Gai, F.; Fehr, M. J.; Petrich, J. W. *J. Phys. Chem.* **1994**, *98*, 5784–5795.

(7) Gai, F.; Fehr, M. J.; Petrich, J. W. *J. Phys. Chem.* **1994**, *98*, 8352–8358.

(8) Fehr, M. J.; Carpenter, S. L.; Petrich, J. W. *Bioorg. Med. Chem. Lett.* **1994**, *4*, 1339–1344.

(9) Fehr, M. J.; McCloskey, M. A.; Petrich, J. W. *J. Am. Chem. Soc.* **1995**, *117*, 1833–1836.

(10) Carpenter, S.; Fehr, M. J.; Kraus, G. A.; Petrich, J. W. *Proc. Natl. Acad. Sci. U.S.A.* **1994**, *91*, 12273–12277.

(11) Kraus, G. A.; Zhang, W.; Fehr, M. J.; Petrich, J. W.; Wannemuehler, Y.; Carpenter, S. *Chem. Rev.* **1996**, *96*, 523–535.

(12) Fehr, M. J.; Carpenter, S. L.; Wannemuehler, Y.; Petrich, J. W. *Biochemistry* **1995**, *34*, 15845–15848.

(13) Das, K.; English, D. S.; Fehr, M. J.; Smirnov, A. V.; Petrich, J. W. *J. Phys. Chem.* **1996**, *100*, 18275–18281.

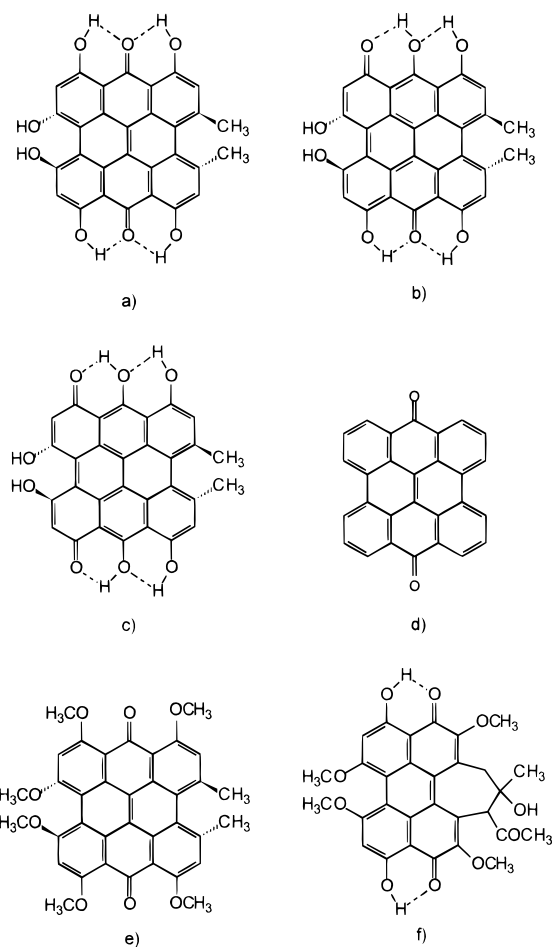


Figure 1. Two-dimensional structures of (a) hypericin, (b) hypericin monotautomer, (c) hypericin bitautomer, (d) mesonaphthobianthrone, (e) hexamethoxy hypericin, and (f) hypocrellin.

lacking labile protons, mesonaphthobianthrone (Figure 1d), is significantly fluorescent and has optical spectra that resemble those of hypericin only when its carbonyl groups are protonated.^{6,7} In hypericin, the fluorescent state grows in on a time scale of several picoseconds, as measured by the rise time of stimulated emission. Therefore, the combined observations of the requirement of protonated carbonyls for strong hypericin-

like fluorescence and the rise time of fluorescence in hypericin was taken as evidence for intramolecular excited-state proton transfer in hypericin.¹⁹ (In this article, we use the term "proton transfer" very loosely. Our current knowledge of the excited state transfer process is not detailed enough to specify whether the process is a proton or an atom transfer.³⁵)

This conclusion initially met with some resistance, despite the precedent set by the large number of organic molecules where the proximity of the enol and keto groups provides an environment that is propitious for excited-state intramolecular proton transfer or hydrogen atom transfer (in this article, we use the two terms interchangeably): for example, malonaldehyde,¹⁴ salicylic acid,¹⁵ 3-hydroxyflavone,¹⁶ benzothiazole,¹⁷ and tropolone¹⁸ are but a few of the examples of a litany of species that execute intramolecular excited-state proton transfer.

One argument proffered against intramolecular excited-state proton transfer in hypericin is the observation of near mirror-image symmetry between its absorption and emission spectra. Such symmetry is typically taken as a signature of negligible structural changes between the absorbing and the emitting species. Intramolecular excited-state proton transfer usually generates a broad structureless emission spectrum that bears little resemblance to the absorbance spectrum. 3-Hydroxyflavone provides a good example.

There are at least two ways to respond to this objection. It is possible that the structural changes induced by proton transfer do not significantly effect the electronic structure of the tautomeric species (Figure 1a–c) in such a way as to destroy the mirror-image symmetry. High-level quantum chemical calculations will have much to offer in understanding this problem. It is also possible, as we have argued elsewhere,^{6,7} that the ground-state of hypericin is already partially tautomerized and that this ground-state heterogeneity yields the observed mirror-image symmetry between absorption and emission spectra.

Here we revisit the questions of ground-state heterogeneity and nonradiative processes. We compare the excited-state transients of hypericin obtained previously using an excitation wavelength of 588 nm^{6,7} with results obtained from a regeneratively amplified and frequency-doubled Ti:sapphire laser providing an excitation wavelength of 415 nm. Changes in the kinetics using different excitation wavelengths is suggestive of ground-state heterogeneity in hypericin. We also present the synthesis of the hypericin analog with no labile protons, hexamethoxyhypericin (Figure 1e, compound **1**), and compare its excited-state transients with those of hypericin. This analog displays *no rise time for stimulated emission*, which we have taken as the signature of intramolecular excited-state proton transfer, and it displays no excited-state transients that can be interpreted in terms of proton transfer.

Experimental Section

A. Synthesis. **i. N,N-Diethyl 2,4-Dimethoxy-6-(hydroxy-3',5'-dimethoxyphenylmethyl)benzamide, 4.** To a solution of TMEDA (1.28 g, 11 mmol) and *s*-BuLi (11 mmol) in 50 mL of THF at $-78\text{ }^{\circ}\text{C}$

(14) Carrington, T., Jr.; Miller, W. H. *J. Phys. Chem.* **1986**, *84*, 4364.

(15) Barbara, P. F.; Walsh, P. K.; Brus, L. E. *J. Phys. Chem.* **1989**, *93*, 29–34.

(16) (a) Brucker, G. A.; Swinney, T. C.; Kelley, D. F. *J. Phys. Chem.* **1991**, *95*, 3190–3195. (b) Strandjord, A. J. G.; Barbara, P. F. *J. Phys. Chem.* **1985**, *89*, 2355–2361. (c) McMorrow, D.; Kasha, M. *J. Phys. Chem.* **1984**, *88*, 2235–2243. (d) Brucker, G. A.; Kelley, D. F. *J. Phys. Chem.* **1987**, *91*, 2856–2861. (e) Schwartz, B. J.; Peteanu, L. A.; Harris, C. B. *J. Phys. Chem.* **1992**, *96*, 3591–3598.

(17) (a) Frey, W.; Laermer, F.; Elsaesser, T. *J. Phys. Chem.* **1991**, *95*, 10391–10395. (b) Laermer, F.; Elsaesser, T.; Kaiser, W. *Chem. Phys. Lett.* **1988**, *148*, 119–124.

(18) Ensminger, F. A.; Plassard, J.; Zwier, T. S.; Hardinger, S. *J. Chem. Phys.* **1993**, *99*, 8341–8344.

was added dropwise amide **2** (2.37 g, 10 mmol) in 15 mL of THF. The mixture was stirred at $-78\text{ }^{\circ}\text{C}$ for 1 h, whereupon aldehyde **3** (1.66 g, 10 mmol) in 15 mL of THF was added dropwise over 5 min. The resulting mixture was stirred at $-78\text{ }^{\circ}\text{C}$ for 1 h. Saturated ammonium chloride solution (20 mL) was added. The solution was diluted with 100 mL of ether and partitioned. The organic layer was separated, washed with water and brine, and dried over MgSO_4 . After concentration in vacuo, the residue was purified by sgc using 4:1 H:EA to provide 3.90 g (97% yield) of **4** as a light yellow oil.

4: NMR (CDCl_3) δ 6.61 (d, $J = 3\text{ Hz}$, 1 H), 6.53 (d, $J = 3\text{ Hz}$, 2 H), 6.50 (d, $J = 3\text{ Hz}$, 2 H), 6.38–6.30 (m, 4 H), 6.26 (t, $J = 3\text{ Hz}$, 1 H), 5.71 (s, 1 H), 5.53 (d, $J = 6\text{ Hz}$, 1 H), 5.35 (d, $J = 9\text{ Hz}$, 1 H), 3.83 (s, 3 H), 3.76 (s, 6 H), 3.74 (s, 3 H), 3.72 (s, 6 H), 3.68 (s, 3 H), 3.68–2.40 (m, 8 H), 1.3–0.75 (m, 12 H); IR (KBr) 3367, 2938, 1602, 1459, 1154, 840 cm^{-1} ; MS (EI) m/e 403, 330 (100), 315, 299, 271, 193; HRMS $\text{C}_{22}\text{H}_{29}\text{O}_6$ calcd 403.19949; measured 403.19919.

ii. 5,7-Dimethoxy-3-(3',5'-dimethoxyphenyl)isobenzofuran-1-one, 5. A solution of **4** (4.00 g, 10 mmol) and pTSA (100 mg) in 200 mL of toluene was heated to reflux for 2 h. The organic solution was washed with 2% sodium bicarbonate, water, and brine and dried. Removal of the solvent by concentration in vacuo yielded 3.27 g (99% yield) of **5** as white crystals (mp 182–184 $^{\circ}\text{C}$).

5: ^1H NMR (CDCl_3) δ 6.39 (m, 4 H), 6.28 (m, 1 H), 6.09 (brs, 1 H), 3.94 (s, 3 H), 3.79 (s, 3 H), 3.73 (s, 6 H); IR (KBr) 2843, 1771, 1600, 1113, 1007, 833 cm^{-1} . ^{13}C NMR (CDCl_3) δ 55.52, 56.03, 56.15, 81.34, 98.38, 99.20, 100.91, 104.70, 106.16, 139.18, 154.68, 159.57, 161.25, 167.02, 168.45; MS (EI) m/e 330 (100), 300, 271, 257, 193, 165; HRMS $\text{C}_{18}\text{H}_{18}\text{O}_6$ calcd 330.11034, measured 330.10952.

iii. 2,4-Dimethoxy-6-(3',5'-dimethoxyphenylmethyl)benzoic acid, 6. A mixture of **5** (300 g, 90 mmol) and 10% Pd/C (500 mg) in 100 mL of ethyl acetate was stirred under a hydrogen atmosphere for 48 h. The suspension was carefully filtered, and the solvent was removed in vacuo. The resulting product was purified by recrystallization from H:EA to provide 278 g (93% yield) of **6** as colorless crystals (mp 163–164 $^{\circ}\text{C}$).

6: ^1H NMR (CDCl_3) δ 6.39 (d, $J = 3\text{ Hz}$, 1 H), 6.36 (d, $J = 2\text{ Hz}$, 1 H), 6.33 (d, $J = 2\text{ Hz}$, 1 H), 6.28 (d, $J = 3\text{ Hz}$, 1 H), 4.23 (br s, 2 H), 3.92 (s, 3 H), 3.75 (s, 3 H), 3.72 (s, 6 H); IR (KBr) 2930, 1694, 1606, 1153, 1081, 844; ^{13}C NMR (CDCl_3) δ 170.32, 162.29, 160.79, 159.24, 144.30, 142.60, 144.30, 142.60, 113.57, 108.31, 107.32, 98.30, 96.82, 56.41, 55.47, 55.31, 40.07; MS (EI) m/e 332, 314, 299, 241, 213, 139; HRMS $\text{C}_{18}\text{H}_{20}\text{O}_6$ calcd 332.12599, measured 332.12572.

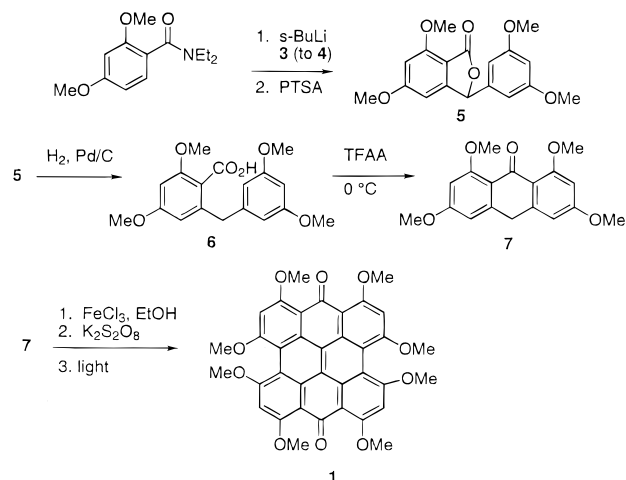
iv. 1,3,6,8-Tetramethoxyanthracen-9-one, 7. To a solution of **6** (1.66 g, 5.0 mmol) in 100 mL of methylene chloride at $0\text{ }^{\circ}\text{C}$ was added trifluoroacetic anhydride (1.05 g, 5.0 mmol) dropwise over 10 min. The solution was stirred at $0\text{ }^{\circ}\text{C}$ for 2 h. Twenty milliliters of methanol was added, followed by 150 mL of 5% sodium bicarbonate. The aqueous layer was extracted with 30 mL of methylene chloride. The combined organic layers were washed with water and brine and dried. After concentration in vacuo, the residue was purified by sgc using 5:1 H:EA to provide 1.41 g (90% yield) of **7** (90% yield) as light yellow crystals (mp 207–208 $^{\circ}\text{C}$).

7: ^1H NMR (CDCl_3) δ 10.65 (s, 1 H), 7.43 (s, 1 H), 6.60 (d, $J = 3\text{ Hz}$, 2 H), 6.29 (d, $J = 3\text{ Hz}$, 2 H), 4.01 (s, 6 H), 3.89 (s, 6 H); IR (KBr) 3319, 2996, 1630, 1578, 1562, 1370, 808; MS (EI) m/e 314 (100), 285, 271, 213, 185, 157; HRMS $\text{C}_{18}\text{H}_{18}\text{O}_5$ 314.11542, measured 314.11554.

v. 1,3,4,6,8,10,11,13-Octamethoxy phenanthro[1,10,9,8-opqra]-perylene, 1. To a solution of anthrone **7** (1.30 g, 4.0 mmol) in 20 mL of boiling EtOH was added a solution of ferric chloride hexahydrate (1.48 g, 5.5 mmol) in 40 mL of EtOH over 10 min. The mixture was heated at reflux for 30 min, cooled, and poured into 600 mL of 5% HCl. The aqueous mixture was extracted three times with 100 mL of EtOAc. The combined organic layers were washed with water and brine and dried over magnesium sulfate.

After the solvent was concentrated in vacuo, the residue was mixed with 5 g of KOH and 100 mL of EtOH and heated to reflux for 5 min. The mixture was cooled to $0\text{ }^{\circ}\text{C}$, and $\text{K}_2\text{S}_2\text{O}_8$ (1.35 g, 15.0 mmol) in 20 mL of water was added dropwise over 5 min at $0\text{ }^{\circ}\text{C}$. The mixture was stirred at ambient temperature for 2 h. The reaction mixture was then poured into 500 mL of 1% HCl and extracted three times with 100 mL of ethyl acetate. The combined organic layers were washed

Scheme 1



with water and brine and dried. After removing the MgSO_4 by filtration, the filtrate was irradiated in a Pyrex flask with a 500 W tungsten lamp for 1 h. The solvent was concentrated in vacuo, and the residue was purified by sgc using 30:1 methylene chloride:methanol to afford 0.78 g (61% yield) of **1** as a red solid (mp 267 °C dec).

1: $^1\text{H NMR}$ (CDCl_3) δ 6.98 (s, 4 H), 4.19 (s, 12 H), 4.13 (s, 12 H). IR (KBr) 2930, 1637, 1540, 1239, 1141, 993 cm^{-1} . MS (ESI) *m/e* 620 (100), 574, 412, 301.

B. Time-Resolved Measurements. Hypericin was used as received from Carl Roth GmbH (distributed by Atomergic Chemetals Corp). DMSO was dried over 4-Å molecular sieves. Care was taken to prevent sieve dust contamination. All experiments were performed at ambient temperature (22 °C). The time-correlated single-photon counting experiments were performed with an apparatus described elsewhere.²⁰ The instrument response function is typically about 70 ps. Hexamethoxy analog samples and hypericin samples were prepared for pump-probe experiments with an optical density of 0.4–0.7 at the pump wavelength; for time-correlated single-photon counting, samples were diluted by 10-fold or more. The time-resolved fluorescence data provide a powerful assay of the purity of the hexamethoxy analog. In addition to a 480-ps decay component, there is a small amount of an \sim 2-ns component whose contribution, possibly a result of oxidation, could be diminished by column chromatography (Figure 7a). Purification, however, did not affect the transient absorption data.

Steady-state fluorescent measurements were made using a Spex Fluoromax with a 4-nm band-pass, and corrections were made for detector response and excitation lamp spectrum. Steady state absorbance measurements were made using a Perkin Elmer Lambda 18 double beam UV–vis spectrophotometer with 1-nm bandpass. The measurement of the fluorescence quantum yield of the hexamethoxy analog was made relative to hypericin by exciting solutions of each compound at several wavelengths where they had equal optical densities and integrating the emission spectrum over the entire band on a wavenumber scale.

The pump probe experiments were carried out on a 2 kHz system based on a Ti:sapphire chirped-pulse regenerative amplifier.²¹ Typical pulse widths were 150 to 200 fs fwhm at 830 nm from autocorrelation measurements. The regenerative amplifier seed pulse train is supplied by a homemade Ti:sapphire oscillator of a Murnane-Kapetyan design.²² The rod is 4.75-mm, and typical pulse widths are sub 20 fs as determined by measurement of the pulse autocorrelation and the spectral

(19) Of special relevance to the role of labile protons for light-induced antiviral activity is the observation that hypericin retains its toxicity in the absence of oxygen and that it acidifies its surroundings upon light absorption.^{8,9,11,12} The retention of toxicity in the absence of oxygen excludes unique assignment of antiviral activity to the trivial generation of singlet oxygen—even though hypericin does generate triplets in high yield.^{25–28}

(20) Gai, F.; Rich, R. L.; Petrich, J. W. *J. Am. Chem. Soc.* **1994**, *116*, 735.

(21) Salin, F.; Squier, J.; Vallincourt, G.; Mourou, G. *Optics Lett.* **1991**, *16*, 1964.

(22) Asaki, M. T.; Huang, C.-P.; Garvey, D.; Zhou, J.; Kapteyn, H. C.; Murnane, M. M. *Optics Lett.* **1993**, *18*, 977.

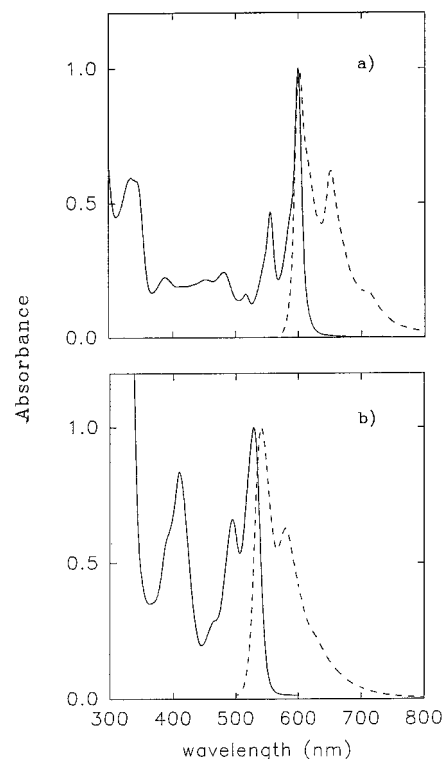


Figure 2. Normalized steady-state absorption (—) and emission (---) spectra of hypericin (a) and hexamethoxyhypericin (b) in DMSO. The excitation wavelength for (a) is 550 nm and for (b) 410 nm.

bandwidth. The output of the amplifier is incident on a beam splitter which sends 56% of the light down a variable delay line and is frequency doubled using a 1-mm BBO crystal. The remaining light traverses a static delay line and is used to create a white light continuum by focusing with a 20-cm lens into a 3-mm thick sapphire flat which is translated to prevent damage. The white light is then passed through the appropriate bandpass filters and split into a probe and reference beam. The pump beam is chopped at 1/2 the repetition rate by a Palo Alto Research Super Chopper 300, which is triggered by the third boxcar averager in the signal processing discussed below. The beams are focused with a 12.5-cm focal length lens and crossed at 36° in a spinning sample holder³³ that rotates at 3400 rpm ensuring a new sample area for every shot. The reference and probe beams are directed into an ISA HR-320 monochromator with a 1200 g/mm grating. The probe and reference beams are detected with Hamamatsu S1336-5BQ photodiodes, which are amplified using Analog Devices op467 precision high-speed OP amps. The outputs are then sent to two Stanford Research SRS250 gated boxcar averagers and subsequently to a Stanford Research SR235 analog processor where the probe signal is divided by the reference to provide a shot-to-shot normalization. The natural log of the quotient is taken and sent to a third boxcar averager, which is operated in toggle mode to provide an active baseline subtraction. Coumarin 500 was probed at 500 nm and used as a standard. Betaine was also used as a standard and compared to previous data collected in a similar fashion.²³ The lower limit of the sensitivity of the detection system was estimated with one scan and without shot-to-shot normalization as a change of 0.016 V in an initial signal of 0.750 V, which corresponds to a worst case limit of a 9.4×10^{-3} change in optical density.

An “artifact” appears frequently in the data and is most evident in the kinetic traces displayed in Figure 3. The “spike” that appears at zero time with either positive or negative sign is a result of the more intense pump pulse modulating the phase of the less intense probe pulse. This phenomenon of cross-phase modulation occurs with pulses of different wavelength and does not require the pulses to be resonant with an absorbing sample.³¹

(23) Johnson, A. E.; Levinger, N. E.; Jarzeba, W.; Schlieff, Ralph E.; Kliner, D. A. V.; Barbara, P. *Chem. Phys.* **1993**, *176*, 555–574.

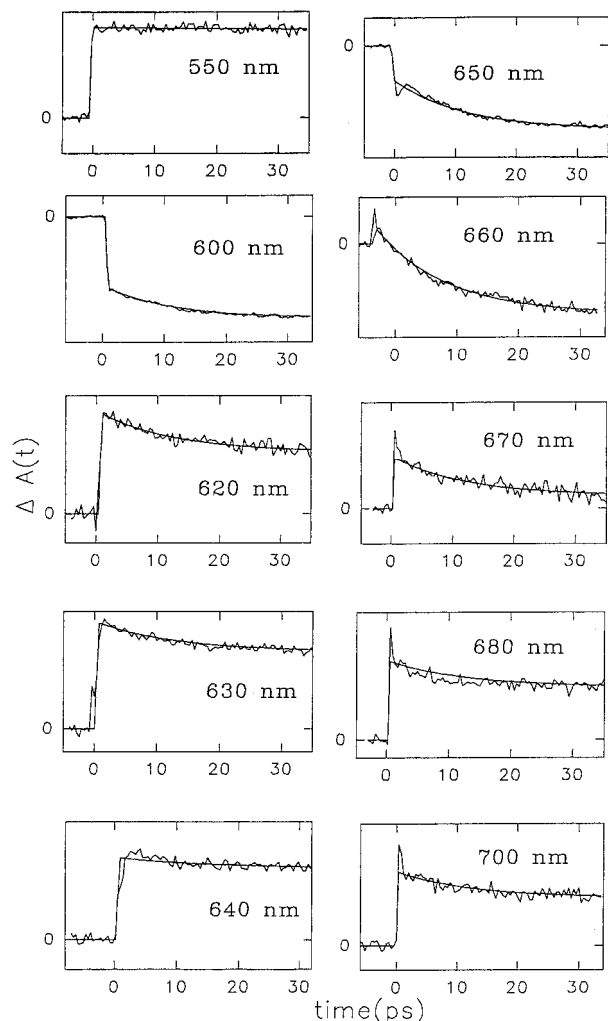


Figure 3. Absorption transients of hypericin in DMSO, $\lambda_{\text{pump}} = 415$ nm; probe wavelengths are indicated in the panels. The “spike” at zero time that is most apparent in the data in this figure is a result of cross-phase modulation of the pump pulse with the probe pulse.³¹ See Experimental Section.

The instrument response of the 30-Hz and 2-kHz systems are determined, respectively, by means of the ground-state bleach of Nile Blue and the stimulated emission of coumarin 500 on a daily basis. On a picosecond time scale, Nile Blue has an instantaneous bleach.^{6,7} On a 100 femtosecond time scale, coumarin 500 in a 1:1 mixture of methanol and water yields stimulated emission at 500 nm with no detectable rise time. These traces are used to approximate the instrument response (the convolution of the laser pulses in the medium) by performing an iterative nonlinear least-squares fit in which a trial instrument response is convoluted with the instantaneous molecular response of the Nile Blue or the coumarin. Several trial instrument response functions are tested until one is found that best fits the rising edge of the data. This function is then used in subsequent analyses until the experiment is either restarted or is known to have changed. The trial functions used are either double-sided exponentials or Gaussians, which have been convoluted with themselves in order to simulate the temporal overlap of two similar pulses in the sample.

Sample preparation for the pump-probe experiments required bubbling argon through the hexamethoxy analog samples and filling the spinning sample holder in a glove bag of argon to reduce oxygen content. This was done after observing rapid degradation of sample in the presence of oxygen. Deoxygenation sufficiently preserved the sample to withstand pump incidence for several hours; without deoxygenation the sample degrades in minutes. Hypericin is stable for hours without deoxygenation and gives the same experimental results in either case.

Kinetic traces acquired at various wavelengths were fit using a global fitting procedure found in Spectra Solve. The global parameters in

Table 1. Global Fitting Parameters^a

hypericin (nm)	a_1	τ_1 (ps)	a_2	τ_2 (ps)	a_3	τ_3 (ps)
550 ^a	0	11.6	1.0	∞	0	
600 ^a	0.30	11.6	-1.0	∞	0	
620 ^a	0.37	11.6	0.63	∞	0	
630 ^a	0.25	11.6	0.75	∞	0	
640 ^a	0.10	11.6	0.90	∞	0	
650 ^b	-0.61	11.6	-0.39	∞	0	
660 ^b	-1.0	11.6	0.27	∞	0	
670 ^a	0.74	11.6	0.26	∞	0	
680 ^a	0.30	11.6	0.70	∞	0	
700 ^a	0.32	11.6	0.68	∞	0	
hexamethoxy hypericin	a_1	τ_1 (ps)	a_2	τ_2 (ps)	a_3	τ_3 (ps)
500 ^c	0	2.5	0.68	480	0.32	∞
510 ^c	0.10	2.5	0.72	480	0.18	∞
515 ^b	0.17	2.5	-0.91	480	0.83	∞
520 ^b	0.10	2.5	-1.2	480	0.90	∞
530 ^a	0	2.5	-3.0	480	1.0	∞
540 ^a	0.11	2.5	-1.2	480	0.89	∞
545 ^d	0	2.5	0.39	480	0.61	∞
580 ^d	0.15	2.5	0.35	480	0.50	∞
630 ^d	0	2.5	0.30	480	0.70	∞

^a The functional form used to fit the data is indicated by a superscript in the leftmost column, which gives the probe wavelength. (a) $\Delta A(t) = a_1 \exp(-t/\tau_1) + a_2 \exp(-t/\tau_2) + a_3 \exp(-t/\tau_3)$. (b) $\Delta A(t) = a_1 [1 - \exp(-t/\tau_1)] + a_2 \exp(-t/\tau_2) + a_3 \exp(-t/\tau_3)$. (c) $\Delta A(t) = a_1 [1 - \exp(-t/\tau_1)] + a_2 [1 - \exp(-t/\tau_2)] + a_3 \exp(-t/\tau_3)$. (d) $\Delta A(t) = a_1 \exp(-t/\tau_1) + a_2 [1 - \exp(-t/\tau_2)] + a_3 \exp(-t/\tau_3)$. The pre-exponential factors are all normalized and should not be interpreted in terms of absolute optical density changes owing to changes in pump intensities and gain settings on data acquisition hardware.

our case were time constants, and local parameters were amplitudes or pre-exponential factors. The time constants are specified, and each curve is fit iteratively varying only the local parameters, that is the amplitudes. A local χ^2 is calculated for each local fit. After all curves are fit, a global χ^2 is calculated as shown below. The global parameters are varied, and the whole process is repeated to calculate a new global χ^2 . This process is repeated until a minimum is reached for χ^2 , which is defined as:

$$\chi^2 = \frac{\sum_{i=1}^n \chi_{\text{local},i}^2}{n}$$

where $\chi_{\text{local},i}^2$ is obtained for each curve letting all parameters local and global (that is amplitudes and time constants) vary, and n is the number of curves. The quality of the fit was determined by visual inspection of the fit and its residuals. The time-resolved absorption/stimulated emission data are displayed in Figures 3–6. The results of the global fits, and the functional forms used to obtain them, are summarized in Table 1.

Results and Discussion

A. Hypericin. i. Rise Time in Stimulated Emission.

Figures 3 and 4a present absorption transients of hypericin in DMSO using excitation wavelengths of 415 and 588 nm, respectively. The changes in signs of the traces in Figure 3 indicate the presence of isosbets for hypericin in the regions 550–600, 600–620, 640–650, and 660–670 nm. The decay times of the absorption transients at probe wavelengths of 620–640 and at 670–700 nm and the rise time of the stimulated emission transients at probe wavelengths of 600 and 650–660 nm are all adequately represented, using a global fitting analysis, by the same time constant of 11.2 ps. This result is consistent with that of 9.2 ps obtained previously using ~ 1 -ps pulses at 588 nm at 30 Hz.^{6,7}

ii. Ground-State Heterogeneity: Excitation Wavelength Dependence. We call attention to the traces obtained using

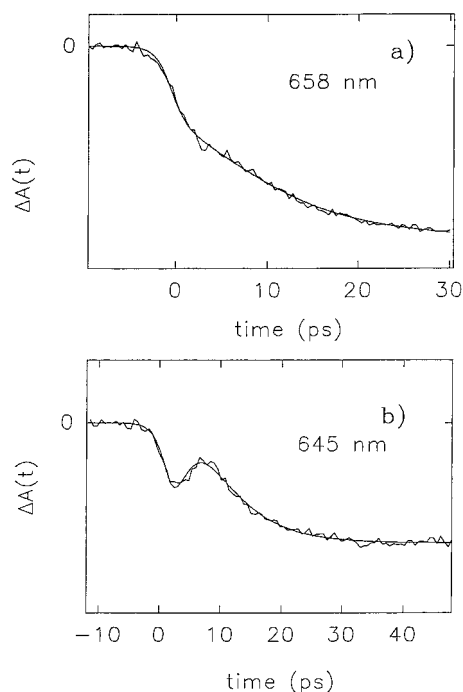


Figure 4. Stimulated emission transients of hypericin, $\lambda_{\text{pump}} = 588$ nm; probe wavelengths are indicated in the panels:⁷ (a) DMSO, $\Delta A(t) = -0.30[1 - \exp(-t/9.2 \text{ ps})] - 0.13 \exp(-t/1.9 \text{ ps})$; and (b) ethylene glycol, $\Delta A(t) = -0.45[1 - \exp(-t/6.4 \text{ ps})] - 0.53 \exp(-t/2.4 \text{ ps})$.

probe wavelengths of 658–660 nm for excitation wavelengths of 415 and 588 nm, respectively (Figures 3 and Figure 4). When hypericin is excited at 588 nm, there is a component of stimulated emission that appears *instantaneously*. This component is absent for excitation at 415 nm. Changes in the kinetics with excitation wavelength is taken to be suggestive of ground-state heterogeneity of the hypericin population. The origin of this apparent heterogeneity may be attributed to various tautomers as well as to different twisted conformations of the aromatic skeleton. See below. (We refer to the heterogeneity as apparent because different laser systems were used to obtain the two results.)

B. Hexamethoxy Hypericin. i. Absence of Stimulated Emission. Figures 5 and 6 present absorption transients of hexamethoxyhypericin in DMSO using an excitation wavelength of 415 nm. Isosbests are apparent at ~ 515 nm and between 540 and 545 nm. The kinetics of hexamethoxyhypericin are simplified with respect to those of hypericin. *No stimulated emission is detected for hexamethoxyhypericin in the region 550–710 nm.* This is not particularly surprising given that we measure its fluorescence quantum yield in DMSO to be only 19%³² that of hypericin. Any weak contribution from stimulated emission is eclipsed by the absorption of excited-state species. What is especially noteworthy, however, is that the transient absorption in the spectral region *where only emission is observed in the steady state*, >610 nm, occurs instantaneously and does not decay on the time scale of the experiment. If there were a component of stimulated emission that appeared *with a finite rise time*, it would manifest itself as an *apparent decay* in the transient absorption signal.

Examination of the steady-state spectra in Figure 2 indicates that the transient at 540 nm arises from a *bleach of the ground-state absorption* and not to a rise time in stimulated emission. The apparent rise time in the bleach, whose time constant is 2.5 ps, must correspond to an excited-state species absorbing at 540 nm and decaying with the same time constant. The rapid

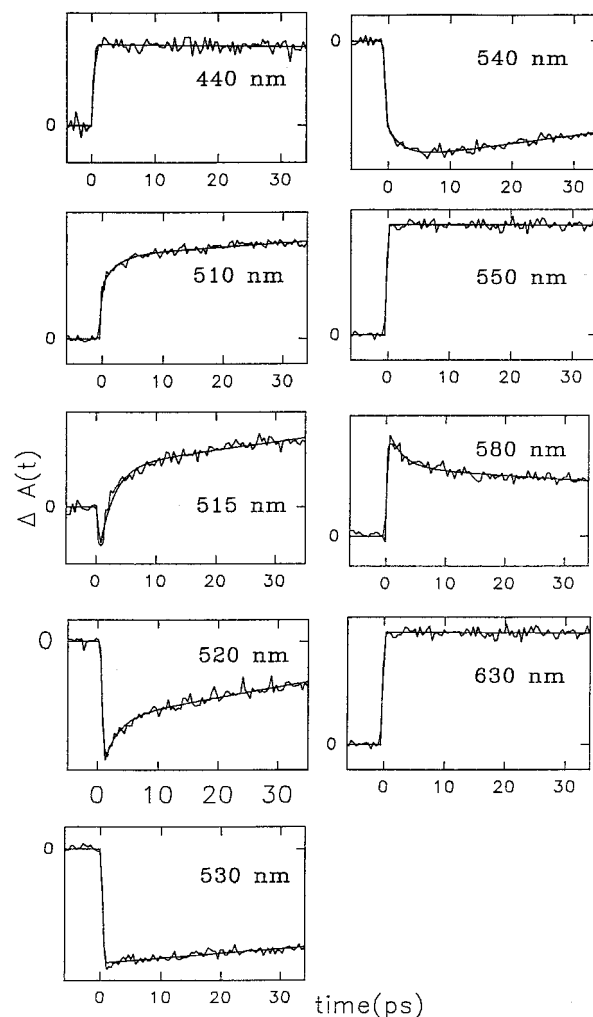


Figure 5. Absorption transients of hexamethoxy hypericin in DMSO, $\lambda_{\text{pump}} = 415$ nm; probe wavelengths are indicated in the panels. The full scale is 40 ps.

transients observed at other probe wavelengths in Figures 5 and 6 clearly resolve a species with this time constant.

We do *not* attribute the 2.5-ps decays observed at 580 and 610 nm to the presence of weak stimulated emission, because a genuine decay of absorbance on this time scale is already consistent with the apparent rise time for the bleach at 540 nm, as discussed above. Furthermore, Figure 5 indicates that in this region there is a component of transient absorption appearing with a 480-ps time constant. This is identical to the fluorescence decay time of hexamethoxyhypericin in DMSO (Figure 7a) and can be interpreted as the formation of triplet species. If the fast transient at 580 and 610 nm in Figure 5 were due to the superposition of a stimulated emission signal on a long-lived absorption signal, it is reasonable to expect that we would also observe simulated emission from the long-lived fluorescence species as well, that is an apparent decay of absorbance of 480 ps. That we do not provides us with additional confidence to conclude that our data provide no evidence of detectable stimulated emission.

ii. Origin of the 2.5-ps Component in Hexamethoxy hypericin. A possible explanation for the presence of the component of transient absorption that decays in 2.5 ps is the combination of internal conversion and dynamic solvation of an excited state of the analog. As the solvent dynamically readjusts itself to the change in the dipole of the solute upon optical excitation, the solute is lowered in energy. This is manifested by the decay of transient absorbance. The dynamic

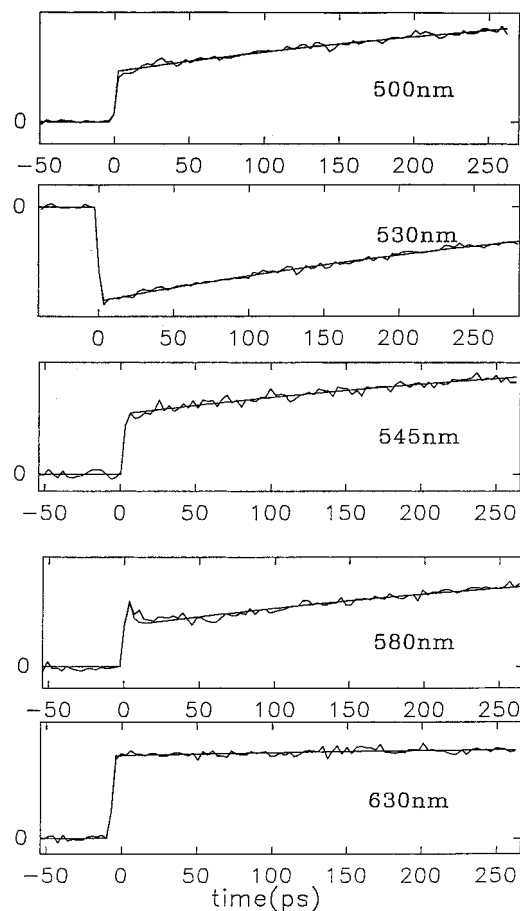


Figure 6. Absorption transients of hexamethoxy hypericin in DMSO, $\lambda_{\text{pump}} = 415$ nm; probe wavelengths are indicated in the panels. The full scale is 320 ps. The slowly rising transient apparent in each panel has a time constant of 480 ps, which matches the fluorescence decay of the analog in DMSO. This transient is attributed to the formation of a triplet species.

solvation time of DMSO is known to be 3 ps.²⁴ It may, of course, be fortuitous that the transient is characterized by an ~ 3 -ps decay; and ideally, a correlation of decay time in various solvents with the known dynamic solvation times would enable us to make this assignment unambiguously. Unfortunately, DMSO is the only solvent in which we are able to dissolve the analog in sufficient quantities to perform these experiments and at the same time avoid sample degradation.

Another possibility for the origin of this component is prompt intersystem crossing to form triplets. We have already noted that the fluorescence quantum yield of hexamethoxy hypericin in DMSO is 19%³² that of hypericin and that hexamethoxyhypericin degrades rapidly when optically excited in the presence of oxygen. These results suggest that the reduced fluorescence quantum yield of this analog may be the result of enhanced intersystem crossing and that the high yield of triplet states effectively generates singlet oxygen, which subsequently destroys it.

In a recent study of the perylene quinone, hypocrellin (Figure 1f), we observe absorption that is produced on the time scale of the fastest kinetic event and have argued that it arises from "prompt" triplet formation.¹³

iii. Rapid Transients in Hypericin and Its Analogs. The stimulated emission kinetics of hypericin in ethylene glycol (Figure 4b) indicate a component that appears instantaneously and decays in ~ 2 ps in addition to the characteristic rise time

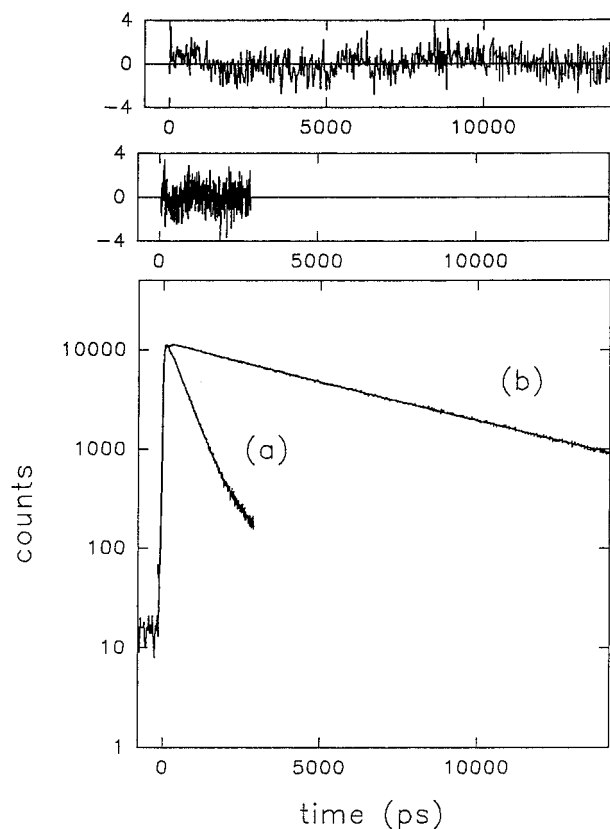


Figure 7. Fluorescence decays obtained from time-correlated single-photon counting at 22 °C. Residuals are displayed at the top of the figure. The topmost set of residuals corresponds to hypericin. (a) Hexamethoxyhypericin in DMSO: $\lambda_{\text{ex}} = 300$ nm, $\lambda_{\text{em}} > 530$ nm; $F(t) = 0.97 \exp(-t/490 \text{ ps}) + 0.03 \exp(-t/2.1 \text{ ns})$, $\chi^2 = 1.15$. The full scale is 3 ns. (b) Hypericin in DMSO: $\lambda_{\text{ex}} = 305$ nm, $\lambda_{\text{em}} > 555$ nm; $F(t) = 1.00 \exp(-t/5.3 \text{ ns})$, $\chi^2 = 1.18$. The full scale is 15 ns. To our knowledge, the fluorescence decay of hypericin and its analogs does not depend on excitation wavelength, visible and ultraviolet excitation yielding similar results.^{6,34} This result should not be confused with the excitation wavelength dependence of the picosecond transients in hypericin indicated in Figures 3 and 4. These transients report on primary processes that are not resolvable in the measurement of the longer lived fluorescence decay.

for stimulated emission that we have attributed to intramolecular proton transfer. One is led to conjecture that the 2.5-ps transient observed at 580–610 nm in hexamethoxyhypericin and the 2-ps transient in hypericin represent prompt intersystem crossing. (By "prompt" intersystem crossing we mean merely to distinguish this process from the slower process occurring with a 480-ps time constant. Presumably these two intersystem crossing rates arise from two different conformational or tautomeric species.) If this is correct, the kinetic scheme postulated for hypericin in Figures 12 and 3 of refs 6 and 7, respectively, needs to be modified. There we proposed that the ~ 2 -ps decay of stimulated emission in hypericin represents the production of a monotaomer (Figure 1b) from the untaomerized species (Figure 1a). The presence of a similar rapid transient in hexamethoxyhypericin, which cannot tautomerize, considered in the context of the above results, suggests that this fast component in hypericin may correspond to ultrafast intersystem crossing.

Conclusions

A procedure has been presented for the synthesis of a crucial analog in the investigation of the hypericin, hexamethoxyhypericin (Figure 1e). Hexamethoxyhypericin has a fluorescence

(24) Barbara, P. F.; Jarzaba, W. *Adv. Photochem.* **1990**, *15*, 1.

quantum yield that is only 19% that of hypericin in DMSO and that exhibits no stimulated emission in DMSO. Based on our previous work on hypericin, these results are consistent with the inability of the hexamethoxy analog to execute an intramolecular excited-state proton transfer.

Hexamethoxyhypericin possesses a rapid component in the decay of its transient absorption (2.5 ps). We suggest that a likely explanation for this component is a combination of dynamic solvation and internal conversion of an excited singlet state higher than S_1 . (Prompt intersystem crossing may also be possible.) We further note that an assignment to intersystem crossing implies that the rapid component (~ 2 ps) of stimulated emission, which is clearly evident in hypericin experiments obtained with excitation wavelengths of 588 nm^{6,7} (Figure 5 part a and especially part b), may also have a similar origin.

An interesting question that requires further study is how does the conformation of the hypericin skeleton influence its electronic structure and its photophysics. The X-ray structures of hypericin³⁰ and hypocrellin²⁹ indicate that they are not planar. (Similar conclusions can be drawn from semiempirical calculations or, more simply, from molecular models.) The large side

chains protruding from the aromatic skeletons repel each other and prevent the molecules from acquiring a planar conformation. This raises the possibility that there are ground-state conformations of hypericin that cannot tautomerize and that, upon optical excitation, undergo ultrafast deactivation by other processes such as internal conversion or intersystem crossing. One can speculate on how distortion of the skeleton in the hexamethoxy derivative affects its spectroscopy: the absorption spectra of the analog and hypericin are qualitatively very similar except for the strong absorption at 400 nm in the analog (Figure 2).

Acknowledgment. D.S.E. was supported by fellowships from Amoco and GAANN. Part of this work was supported by NSF Grants BIR-9413969 and CHE-9613962 to J.W.P. and by a grant from the Center for Advanced Technology and Development to G.A.K.

JA962476H

(25) Racinet, H.; Jardon, P.; Gautron, R. *J. Chim. Phys.* **1988**, *85*, 971–977.

(26) Eloy, D.; Le Pellec, A.; Jardon, P. *J. Chim. Phys.* **1996**, *93*, 442–457.

(27) Diwu, Z.; Lowen, J. W. *Free Radical Biol. Medicine* **1993**, *14*, 209–215.

(28) Malkin, J.; Mazur, Y. *Photochem. Photobiol.* **1993**, *57*, 929–933.

(29) Wei-shin, C.; Yuan-teng, C.; Xiang-yi, W.; Friedrichs, E.; Puff, H.; Breitmaier, E. *Liebigs Ann. Chem.* **1981**, 1880–1885.

(30) (a) Etlzstorfer, C.; Falk, H.; Müller, N.; Schmitzberger, W.; Wagner, U. G. *Monatsh. Chem.* **1993**, *124*, 751–761. (b) Falk, H. Personal communication. (c) Freeman, D.; Frolow, F.; Kapinus, E.; Lavie, D.; Lavie, G.; Meruelo, D.; Mazur, Y. *J. Chem. Soc. Chem., Commun.* **1994**, 891–892.

(31) Diels, J.-C.; Rudolph, W. *Ultrashort Laser Pulse Phenomena*; Academic Press: San Diego, 1996; p 142.

(32) Because this number is obtained from a steady-state measurement, which does not discriminate against the 2-ns impurity or degradation product (Figure 7a), it overestimates the fluorescence quantum yield of the analog. The decrease in fluorescence quantum yield of the analog is more clearly apparent in the decay of its excited singlet state: in DMSO, it possesses a fluorescence decay of 500 ps, as opposed to 5 ns for that of hypericin (Figure 7). Consequently, a large component of the triplet population in hexamethoxyhypericin is expected to appear with a 500 ps time constant, as is observed in Figure 6.

(33) Savikhin, S.; Wells, T.; Song, P.-S.; Struve, W. S. *Biochemistry* **1993**, *32*, 7512.

(34) Yamazaki, T.; Ohta, N.; Yamazaki, I.; Song, P.-S. *J. Phys. Chem.* **1993**, *97*, 7870.

(35) Das, K.; English, D. S.; Petrich, J. W. *J. Am. Chem. Soc.* **1997**, in press.